

# Simulation of metal oxide surge arrester dynamic behavior under fast transients

A. BAYADI<sup>1</sup>, N. HARID<sup>2</sup>, K. ZEHAR<sup>1</sup>, S. BELKHIAT<sup>1</sup>

(1) Université Ferhat Abbas Sétif, Faculté des sciences de l'ingénieur, Département d'électrotechnique  
Algeria (e-mail : a\_bayadi@yahoo.fr, dpt\_electrotechnique@arn.dz)

(2) Cardiff School of Engineering, Engineering Electrical Division Cardiff, United Kingdom  
(e-mail : haridn@cardiff.ac.uk)

**Abstract** – Data on characteristics of metal-oxide surge arresters indicates that for fast front surges, those with rise times less than 8µs, the peak of the voltage wave occurs before the peak of the current wave and the residual voltage across the arrester increases as the time to crest of the arrester discharge current decreases.

Several models have been proposed to simulate this frequency-dependent characteristic. These models differ in the calculation and adjustment of their parameters.

In the present paper, a simulation of metal oxide surge arrester (MOSA) dynamic behavior during fast electromagnetic transients on power systems is done. Some models proposed in the literature are used.

The simulations are performed with the Alternative Transients Program (ATP) version of Electromagnetic Transient Program (EMTP) to evaluate some metal oxide surge arrester models and verify their accuracy.

**Keywords** – Metal Oxide Surge Arrester, ATP-EMTP, Modeling, Electromagnetic fast Transients, Power systems, lightning, Induced overvoltages, Simulation, parameter Estimation, Insulation coordination, measurements.

## I. INTRODUCTION

The metal oxide arrester protects the insulation of equipments in electrical systems against internal and external overvoltages. They exhibit an extremely high resistance during normal operation and a very low resistance during transient overvoltages. That is, the (V-I) characteristic of the device is non-linear [1, 2, 3, 4].

The highly non-linear V-I characteristic obviates the need for series spark gaps. The electrical characteristics are determined solely by the properties of the metal oxide blocks. MO surge arresters with spark gaps are still marketed by several manufacturers for medium voltage applications.

Data on characteristics of metal-oxide surge arresters indicates that these devices have dynamic characteristics that are significant for overvoltage coordination studies involving fast front surges and for their location. For fast front surges, those with rise times less than 8µs, the peak of the voltage wave occurs before the peak of the current wave and the residual voltage across the arrester increases as the time to crest of the arrester discharge current decreases. This increase of the residual voltage could reach approximately 6% when the front time of the discharge current is reduced from 8 to 1.3 µs [5, 6, 7]. Indeed, the voltage across the arrester is not only a function of the discharge current, but also of the rate of its rise. This will not be the case if the metal-oxide performed strictly as a non-linear resistance [4]. Therefore, this frequency-

dependent behavior, require a more sophisticated model than the simple static non-linear resistance.

Several models [5, 6, 7, 8, 9, 10, 11] have been proposed to simulate this frequency-dependent characteristic. Difficulties arise in the calculation and adjustment of their parameters: in some cases iterative procedures are required, in others the necessary data are not reported on manufacturers' datasheets. These models differ in the calculation and adjustment of their parameters but they have an acceptable accuracy as reported in the literature.

## II. CONVENTIONAL OR NON-LINEAR RESISTOR MODEL

A non-linear resistor will not have the same voltage and current shape when operated in the non-linear domain. The interesting surge arrester model available in the EMTP program is the exponential non-linear resistive device (fig. 1) [12,13].

The Type-92 seems to be free of any serious limitations or deficiencies. In this model the V-I characteristic can be represented by an arbitrary number of exponential segments, where each segment has constraint equation defined by:

$$i = P \left( \frac{v}{V_{ref}} \right)^q \quad (1)$$

Where:

i, v are the arrester current and voltage respectively;

p, q and Vref are constants of the device.

We note that Vref is an arbitrary reference voltage that normalizes the equation and prevents numerical overflow during exponentiation. Then constants p and q are unique parameters of the device. The first segment of the device is linear, which avoids possible numerical underflow and speeds the simulation. But the dynamic behavior mentioned previously is anymore reproduced by this model

## III. MODEL PROPOSED BY TOMINAGA ET AL

In reference [11] Tominaga et al have proposed a simple model (fig. 2) to include the dynamic characteristic similar to hysteresis effect, through the addition of a series inductance L, whose value can be estimated once the arrester current is approximately known from a trial run. This approach had some merit because the voltage across the inductance, and hence across the arrester, would increase as the time to crest of the current decreased. This type of model had some success in matching a particular test result. For example, an inductance could be chosen for the model such that it gave a reasonably good match of the

voltage magnitude and waveshape for an arrester discharge current which reached its crest in 8  $\mu$ s. However, when the same inductance and other model parameters were used for an arrester discharge current which reached its crest in 1  $\mu$ s, the voltage magnitude was in error by a significant amount. Different parameters could be chosen for the model such that good results could be obtained for the voltage corresponding to an arrester current reaching its crest in 1  $\mu$ s. However, if the time to crest of the current differed very much from 1  $\mu$ s, the resulting voltage was in error.

#### IV. MODEL PROPOSED BY KIM I. ET AL

The proposed [7] non linear inductance model of a ZnO arrester is shown in fig. 3. It consists of a non-linear inductance in series with a non linear resistance. As mentioned by the authors this model provide a good response characteristic to steep front wave impulse calculation. This model need a computer program to calculate the non linear inductance characteristic and it needs a relatively big number of voltage-current points which are not usually found in the manufacturer's datasheets

#### V. MODEL PROPOSED BY SCHMIDT ET AL

Based on their experimental results, the author have developed a model for an arrester block shown in fig. 4

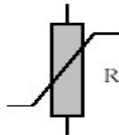


Fig. 1 Non linear resistor model [12]

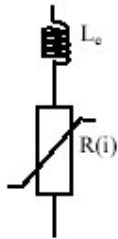


Fig. 2 Linear inductance model [11]

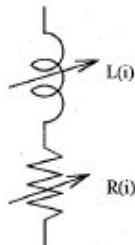


Fig. 3 Non linear inductance model [7]

As mentioned by the author [5], this circuit is able to describe the observed phenomena. The turn-on element A in the equivalent circuit is evaluated from the results of the measurements obtained with the RLC circuit. The other parameters were evaluated from independent measurements or from results described in the literature. The elements R and L are attributed to the ZnO grain, whereas the other elements are related to the grain boundaries.

The non-linear resistance consists of the non-linear effect at the grain boundary and the linear resistance of the ZnO grain.

The turn-on element A which will account for the dynamic charge distribution at the grain boundary. This a function of voltage, rate of rise of voltage and the time constant T for reaching the equilibrium of electrons and holes at the grain boundary.

An inductance of 1 $\mu$ H/m was assumed. The simulation of the equivalent circuit resulted in an excellent fit to experiment despite the use of data of other investigators to determine the components of the model. Because care must be taken when using other's works in order to achieve an accurate simulation.

#### VI. MODEL PROPOSED BY HADDAD ET AL

The proposed equivalent circuit [9] is shown in fig. 5. It comprises two series sections; one to represent the resistance of zinc oxide grains ( $R_{\text{grain}}$ ) and the self inductance ( $L_{\text{body}}$ ) due to the physical size of the arrester body and a parallel network to represent the properties of the intergranular layers. One branch of the network carries the high amplitude discharge current, so that the ranch has a highly non-linear resistance  $R_{\text{lg}}$  and a low value inductance  $L_{\text{c1}}$ . The second branch has a linear resistance  $R_{\text{c}}$  and a higher value inductance  $L_{\text{c2}}$  to account for the delay in low-current fronts and the multiple-current path concept. A capacitive element  $C_{\text{lg}}$  to represent the arrester shunt capacitance was also included in the equivalent network. The simulation of the model resulted in an excellent fit to experiment conducted in the laboratory despite that the model parameters are determined experimentally which is sometimes difficult to achieve.

#### VII. THE IEEE RECOMMENDED MODEL

A model [6], which can represent the effects mentioned previously over this range of times to crest, is shown in Fig. 6. In this model the non-linear V-I characteristic is represented with two sections of non-linear resistances designated  $A_0$  and  $A_1$ . The two sections are separated by an R-L filter. We have two situations:

1. For slow-front surges, the impedance of the R-L filter is extremely low leading to consider that the two non-linear resistors of the model are practically connected in parallel.
2. For fast-front surges, the impedance of the R-L filter becomes more important. By this fact the high frequency currents are forced by the RL filter to flow more in the non-linear section designated  $A_0$  than in the section designated  $A_1$ . Since characteristic  $A_0$  has a higher voltage

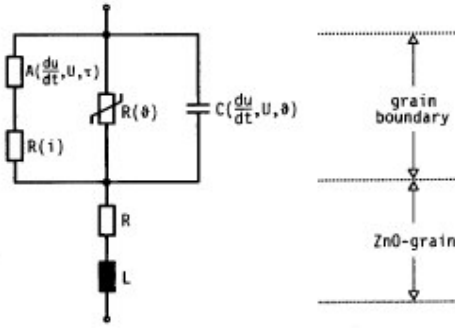


Fig. 4 Model proposed in [5]

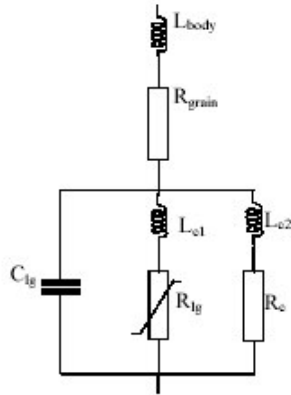


Fig. 5 Model proposed in [9]

for a given current than  $A_1$ , the result is that the arrester model generates a higher voltage.

The inductance  $L_0$  represents the inductance associated with the magnetic fields in the immediate vicinity of the arrester. The resistor  $R_0$  is used to avoid numerical instability when running the model with a digital program. The capacitance  $C_0$  represents the external capacitance associated to the height of the arrester.

### VIII. MODEL PROPOSED BY PINCETI ET AL

The model presented by the authors derives from the IEEE recommended model of the previous section, with some minor differences [8]. This model is shown in fig. 7.

1. The capacitance is eliminated due to its little effect on the model behavior
2. The two resistances in parallel with the inductances are replaced by one resistance  $R$  (about  $1M\Omega$ ) between the input terminals; this resistance has the only scope to avoid numerical troubles. The operating principle is quite similar to that of the IEEE recommended model.

### IX. MODEL PROPOSED BY FERNANDEZ ET AL

The proposed model is shown in fig. 8 and derives from that in [6]. It is intended for the simulation of the dynamic characteristics for discharge currents with front times starting from  $8\mu s$ . Between the non-linear resistances  $A_0$

and  $A_1$  only the inductance  $L_1$  is taken into account.  $R_0$  and  $L_0$  are neglected.  $C_0$  represents the terminal-to-terminal capacitance of the arrester. The resistance  $R$  in parallel to  $A_0$  is intended to avoid numerical oscillations. The model in figure 3 works essentially in the same way as that proposed in [6].

### X. IMPLEMENTATION OF THE MODELS

Some of the models presented in previous sections were implemented in the EMTP via the ATPDraw preprocessor [14, 15]. These circuits permit us to simulate the behavior of each arrester model with different current impulses. In this study the simulations considered discharge tests with fast current impulses ( $1/2\mu s$  wave) and lightning current impulses ( $8/20\mu s$  wave) with amplitudes ranging between 1 kA and 40 kA.

The models were built to a 3kV GE Tranquell arrester, which has an overall height of 0.485m and a switching surge discharge voltage of  $V_{ss}=6.3kV$  for a surge current of 0.5kA, 45 $\mu s$  time to crest [16]. The technical data are reported in table I.

### XI. SIMULATION RESULTS

The simulations were performed with the Alternative Transient Program (ATP). The peak voltages and times to crest of each model for the ( $1/2\mu s$ ) and ( $8/20\mu s$ ) are presented in table II. In this table "FS" means fast surge, "LS" lightning surge, "Man" means the manufacturer's data obtained from catalogues, "Vr" maximum residual voltage in kV, "Tc" time to crest in  $\mu s$  and " $\epsilon_r$ " is the

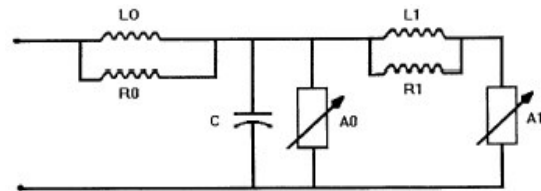


Fig.6 Model proposed in [6]

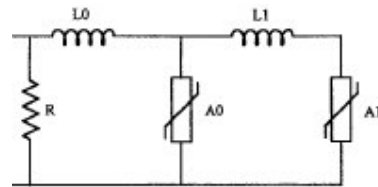


Fig. 7 Model proposed in [8]

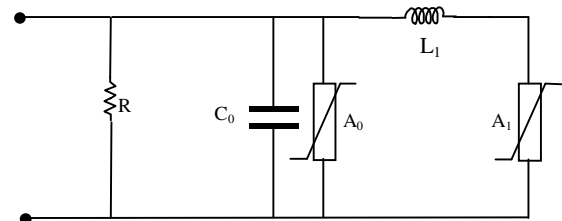


Fig. 8 Model proposed in [10]

relative error in % defined by:

$$\epsilon_r = \frac{V_{rsim} - V_{rman}}{V_{rman}} \times 100 \quad (2)$$

where:

$V_{rsim}$  : is the simulated residual voltage;

$V_{rman}$  : is the manufacturer's residual voltage.

The waveforms results are presented in figs. 9 (a), 9 (b), 10 (a) and 10 (b).

The 1/2  $\mu$ s impulse calculation results are presented in fig. 9 (a) for current amplitude of 10kA.

In this case (fast impulse calculation), for the conventional model calculation, the residual voltage and the discharge current attain their maximum at the same time; the dynamic behavior is anymore reproduced. This is due to the fact that this model is built only with a non-linear resistance. But for the other models the maximum residual voltage occurs before the discharge current peak and the time to maximum voltage is shorter than the time to

Table I Technical data for 3kV Tranquell arrester.

Rated Voltage kVrms	MCOV kVrms	0.5 $\mu$ sec 10kA Max IR-kVcrest	Switching Surge Maximum IR-kVcrest		
3	2.55	9.1	6.3		
8/20 Maximum Discharge Voltage – kVcrest					
1.5 kA	3 kA	5 kA	10 kA	20 kA	40 kA
6.9	7.2	7.5	8.0	9.0	10.3

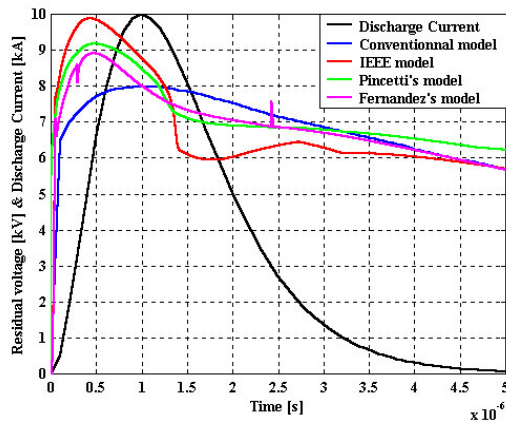


Fig. 9 (a). 10kA, 1/2  $\mu$ s Impulse current wave

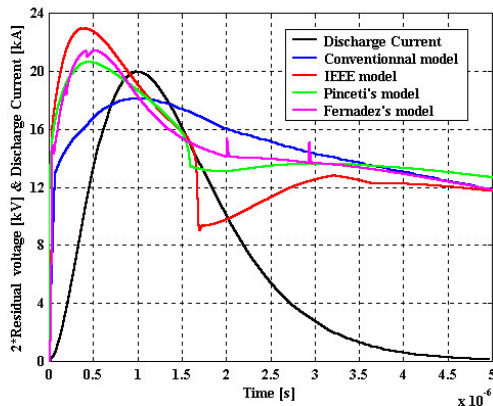


Fig. 9 (b). 20kA, 1/2  $\mu$ s Impulse current wave

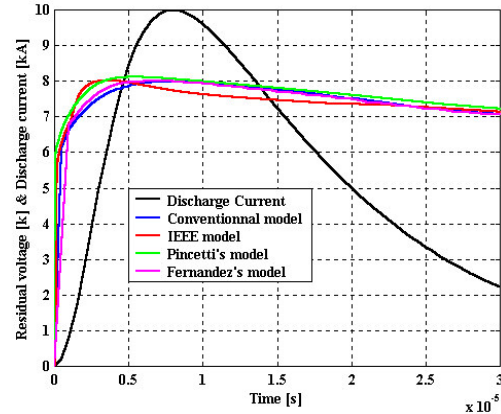


Fig. 10 (a). 10kA, 8/20 $\mu$ s Impulse current wave

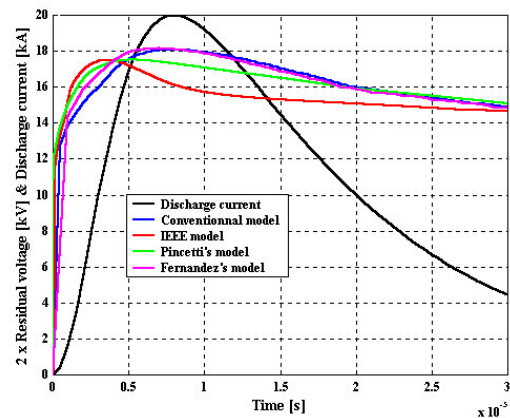


Fig. 10 (b). 20kA, 8/20 $\mu$ s Impulse current wave

maximum current of about 0.57 $\mu$ s for the IEEE model, 0.51 $\mu$ s for Pincetti's model and 0.52 $\mu$ s for Fernandez's respectively. In steep front impulse the time to crest voltage of the manufacturer's data is shorter than the time to maximum current by 0.5 $\mu$ s, and then it seems be satisfactory simulation results in comparison with the manufacturer's data. Regarding the amplitudes the conventional model and the IEEE recommended model produced a greatest error of about 12.2% for the first and 8.46% for the last.

The relative error does not exceed 2.6% for the other models as shown in table II. In figure 9 (b) we present the same test but with current amplitude of 20kA and the same remarks can be made. In the case of Fernandez's model, the voltage peaks on the residual voltage waveforms are due to numerical errors associated perhaps with the constant time step used by the EMTP package but we also note that a good choice of this time step may eliminate or minimize this errors.

We also show in fig. 11 the dynamic hysteresis curve associated with the conventional model. As can be seen the area of the hysteresis loop is practically negligible leading to confirm the absence of the dynamic behavior in that case.

In the contrary when we check the dynamic hysteresis curve associated with IEEE, Pincetti's and Fernandez's

Table II Calculated residual voltages for the 3kV arrester

Type of surge	FS	LS						
Current (kA)	10	1.5	3	5	10	20	40	
Man								
Model	9.1	6.9	7.2	7.5	8.0	9.0	10.3	
Conv	V <sub>r</sub>	7.99	6.90	7.20	7.52	7.99	9.05	10.27
	T <sub>c</sub>	1.0	8.0	8.0	8.0	8.0	8.0	8.0
	e <sub>r</sub>	-12.2	0.00	0.00	0.27	-0.12	0.56	-0.29
[6]	V <sub>r</sub>	9.87	6.87	7.32	7.57	8.01	8.77	9.82
	T <sub>c</sub>	0.43	7.56	5.43	4.50	3.88	3.50	3.39
	e <sub>r</sub>	8.46	-0.44	1.67	0.93	0.12	-2.56	-4.66
[8]	V <sub>r</sub>	9.17	7.09	7.38	7.67	8.11	8.74	9.53
	T <sub>c</sub>	0.49	7.50	6.89	6.67	5.54	5.45	7.73
	e <sub>r</sub>	0.77	2.75	2.50	2.27	1.38	-2.89	7.48
[10]	V <sub>r</sub>	8.87	6.90	7.20	7.52	8.01	9.08	10.37
	T <sub>c</sub>	0.48	7.71	7.98	7.24	6.66	6.89	5.94
	e <sub>r</sub>	-2.53	0.00	0.00	0.27	0.13	0.89	0.68

model which are presented in figure 12, 13, 14 one can easily see that the area of this hysteresis loop is very important which confirm the observed time lag between the residual voltage and the discharge current.

Lightning current impulses (8/20 $\mu$ s wave) calculation results are presented in figure 10 (a) with amplitude 10kA. From this figure all models produce relatively the same residual voltage waveforms and have sufficient accuracy ranging from 0.00% to 2.89% for different current amplitudes (table II). Also we shall note that only the conventional model which does not reproduce the dynamic effect for this range of time to crest (fig. 11). But for dynamic hysteresis curve associated with IEEE, Pincetti's and Fernandez's model which are presented in figs. 12, 13, 14 one can easily see that the area of this hysteresis loop in that case is relatively small compared with the case of fast impulse tests which is in accordance with the time lag observed in fig. 10 (a). The same test is applied but for current amplitude of 20kA and the simulations results are depicted in fig. 10 (b). The same remarks can be made.

From table II, we note that for (40kA, 8/20 $\mu$ s) wave the Pincetti's model draw an error of about 7.48% in this case.

## XII. CONCLUSIONS

In this work, a simulation of the dynamic behavior of metal oxide surge arrester models associated with fast impulse tests was done. The simulations were performed with the Alternative Transient Program version of the Electromagnetic Transients Program (ATP-EMTP). The modeling results compared with the data reported on the manufacturer's catalogue were given to demonstrate the MOSA'S models accuracy. It has been shown that the frequency dependant models proposed in [8, 10] reproduce acceptably the peak voltages from manufacturer while the conventional and the IEEE present a relatively high error. Regarding the occurrence of the voltage maximum before the current maximum, only the conventional model that does not reproduce this effect and the two maximum occur at the same time. The other models are in agreement with

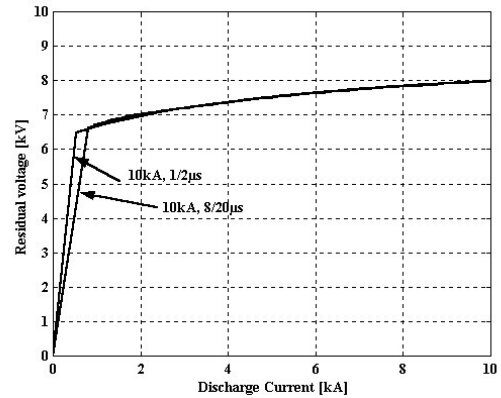


Fig. 11 Dynamic behavior of the conventional model

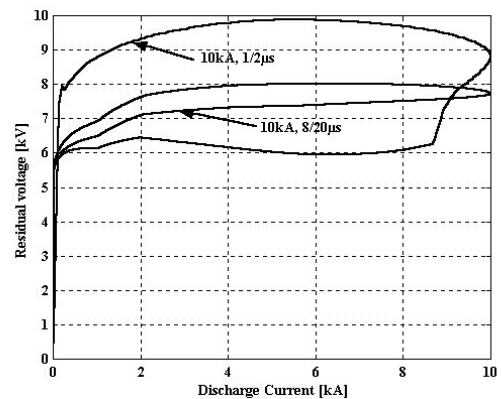


Fig. 12 Dynamic behavior of the IEEE model

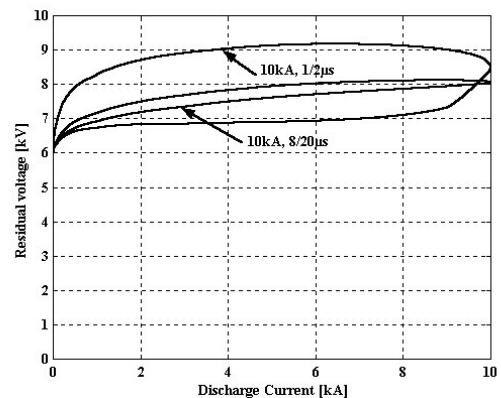


Fig. 13 Dynamic behavior of the Pincetti's model

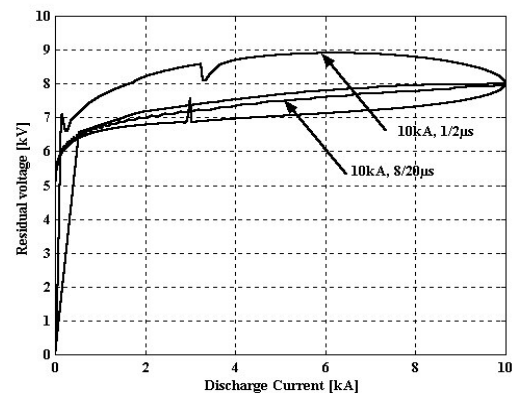


Fig. 14 Dynamic behavior of the Fernandez's model

the manufacturer's catalogue. Finally, we note that for the case of relatively slow surges only the conventional model suffice.

[16] General Electric Company, "TRANQUELL® Surge Arresters, Product Selection & Application Guide", GE Arresters datasheets, 2001.

#### REFERENCES

[1] L. Stenström et al, 'Design and testing of polymer housed surge arrester', GCC CIGRÉ 9<sup>th</sup> Symposium, Abu Dhabi, October, 19p, 1998.

[2] 'IEEE Guide for the Application of Metal -Oxide Surge Arresters for Alternating-Current Systems', IEEE Std C62.22-1991.

[3] A. BAYADI, 'Protection d'un poste de transformation 220kV contre les surtensions de foudre', Conférence Maghrébine sur le Génie Electrique, CMGE'01, Université de Constantine, Algérie, 05-06 Novembre 2001.

[4] A. BAYADI, 'Using metal oxide surge arrester models for power system transients studies', Paper accepted in the Conference on Electrical Engineering, CEE'02, University of Batna, Algeria 10-11 December 2002

[5] W. Schmidt, J Meppelink, B. Richter, K. Feser, L. Kehl and D. Qiu, 'Behavior of MO - surge arrester blocks to fast transients', IEEE Transactions on Power Delivery, Vol. 4, N° 1, pp. 292-300, 1989.

[6] IEEE Working Group 3.4.11, 'Modeling of metal oxide surge arresters', IEEE Transactions on Power Delivery, Vol. 7, N° 1, pp. 302-309, 1992.

[7] Kim, I.; Funabashi, T.; Sasaki, H.; Hagiwara, T.; Kobayashi, M.; 'Study of ZnO arrester model for steep Front Wave', IEEE Transactions on Power Delivery, Vol. 11, N°2, April pp. 834-841, 1996.

[8] P. Pinceti, M. Giannettoni, 'A simplified model for zinc oxide surge arresters', IEEE Transactions on Power Delivery, Vol. 14, N° 2, pp.393-398, 1999.

[9] A. Haddad and P. Naylor, 'Dynamic response of ZnO arresters under high amplitude fast impulse currents', International power electric conference, pp. 292-297, 1999.

[10] Fernandez F., Diaz R., 'Metal oxide surge arrester model for fast transient simulations' paper 144, International conference on power system transients, IPST'01, 20 -24 June 2001.

[11] S. Tominaga, K Azumi, Y. Shibuya, M. Imataki, Y. Fujiwara and S. Nichida, 'Protective performance of metal oxide surge arrester based on the dynamic v-i characteristics', IEEE Trans. Power App. Syst., Vol. PAS-98, pp. 1860-1871, 1979.

[12] Leuven EMTP Center (LEC), 'Alternative Transients Program Rule Book', V.E, 'Exponential ZnO surge arrester R(i)', 1987.

[13] Leuven EMTP Center (LEC), 'Alternative Transients Program Rule Book', XIX.I, 'ARRDAT to punch type-92 Branch cards for ZnO Surge arrester' , 1987.

[14] Alternative Transient Program Rule Book, Can/Am EMTP User Group, USA, 1997.

[15] Prikler, L., Høidalen, H-K.: ATPDraw version 3.5 for Windows9x/NT/2000/XP-User's Manual, SINTEF Energy Research AS, Norway, TR F5680, ISBN 82-594-2344-8, Aug 2002